Chapter 10

TRANSVERSE INSTABILITIES

10.1 Transverse Focusing and Transverse Wake

Transverse focusing of the particle beam is necessary. If not the beam will diverge hitting the vacuum chamber and get lost. The alternating gradient focusing scheme suggested by Courant and Synder [1] employs F-quadrupoles and D-quadrupoles to provide for strong focusing of the beam in both the horizontal and vertical planes. For this reason, the transverse beam size can be made very small and so is the size of the vacuum chamber and the aperture of the magnets. In light sources, usually the Chasman-Green lattices are used. They consist of double achromats or triple achromats, which are strong focusing and give zero dispersion at both ends. Another merit of the achromats is that they can provide much smaller transverse emittances for the electron beam than the alternating gradient scheme of Courant and Synder.

Because quadrupoles can focus in only one transverse plane and defocus in the other, transverse oscillations develop in both transverse planes. These are called *betatron oscillations*, and the oscillation frequencies, $\omega_\beta/(2\pi)$, are called *betatron frequencies*, which are usually different in the two transverse planes. The number of betatron oscillations made in a revolution turn of the beam, $\nu_\beta = \omega_\beta/\omega_0$, is called the *betatron tune*. The equation of motion of a beam particle in, for example, the vertical plane, is given by

$$\frac{d^2y}{dn^2} + (2\pi\nu_\beta)^2 y = \frac{C^2\langle F_1^\perp\rangle}{\beta^2 E_0} \ , \tag{10.1}$$

where n denotes turn number and the right side is the contribution due to the transverse electromagnetic wake $W_1(\tau)$. Consider a coasting beam with current I_0. The transverse force averaged over the circumference of the ring, $\langle F_1^\perp \rangle$ acting on the test particle is related to the transverse impedance through Eqs. (1.26) to (1.28):

$$Z_1^\perp = -\frac{iC\langle F_1^\perp \rangle}{e\beta I_0 \bar{y}} \tag{10.2}$$

where $\bar{y}$ is the transverse displacement of the beam center. After averaging over all the beam particles, we obtain the equation of motion for the transverse motion of the beam center:

$$\frac{d^2\bar{y}}{dn^2} + (2\pi\nu_\beta)^2\bar{y} = \frac{ie\beta I_0 Z_1^\perp C}{\beta^2 E_0}\,\bar{y}\ . \tag{10.3}$$

Thus, the transverse wake amounts to a betatron frequency shift

$$\Delta\omega_\beta = -\frac{i\beta c^2}{2\omega_\beta E_0}\,\frac{I_0}{C}\,Z_1^\perp\ , \tag{10.4}$$

where c is the velocity of light. For a coasting beam, transverse excitation comes from the transverse impedance that samples one or more of the betatron sidebands $n\omega_0 + \omega_\beta$ flanking the revolution harmonic n. The reactive part of $Z_1^\perp(\omega)$ produces a real frequency shift. The resistive part of the impedance produces an imaginary frequency shift, which if positive implies instability. Since $\mathcal{R}e\, Z_1^\perp(\omega) \gtrless 0$ when $\omega \gtrless 0$, the resistive part causes instability for negative frequency. Therefore only coasting-beam modes with $n < -\nu_\beta$ can be unstable.

There is a direct parallel between the transverse dynamics and the longitudinal dynamics, as is illustrated in the equations of motion in the longitudinal phase plane and the transverse phase plane. However, there is a big difference that the betatron tune $\nu_\beta \gg 1$ while the synchrotron tune $\nu_s \ll 1$.

10.2 Separation of Transverse and Longitudinal Motions

Just as for synchrotron oscillations, it is more convenient to change from (y, p_y) to the circular coordinates (r_β, θ) in the transverse betatron phase space. Following Eq. (7.1), we have

$$\left\{\begin{aligned} y\ &= r_\beta \cos\theta \\ p_y &= r_\beta \sin\theta\ , \end{aligned}\right. \tag{10.5}$$

and Eq. (10.1) is transformed into

$$\begin{cases} \dfrac{dy}{ds} &= -\dfrac{\omega_\beta}{v} p_y \\ \dfrac{dp_y}{ds} &= \dfrac{\omega_\beta}{v} y - \dfrac{c}{E_0 \omega_\beta \beta} \langle F_1^\perp(\tau; s) \rangle \ , \end{cases} \tag{10.6}$$

where instead of turn number, the continuous variable s, denoting the distance along the designed orbit, has been used as the independent variable.

For a bunched beam, longitudinal motion has to be included. For time period much less than the synchrotron damping time, Hamiltonian theory can be used. The Hamiltonian for motions in both the longitudinal phase space and transverse phase space can be written as

$$H = H_{||} + H_\perp \ , \tag{10.7}$$

where $H_{||}$ is the same Hamiltonian describing the longitudinal motion:

$$H_{||} = -\frac{\eta(\Delta E)^2}{2 v_0 \beta_0^2 E_0} - \frac{eV_{\rm rf}}{C_0 h \omega_0}\Big[\cos(\phi_s - h\omega_0\tau) - \cos\phi_s - h\omega_0\tau\sin\phi_s\Big] + V(\tau)\Big|_{\rm wake}, \tag{10.8}$$

while $H_\perp$ is the additional term coming from the equations of motion in the transverse phase space as given by Eq. (10.6). Note that the transverse force $\langle F_1^\perp(\tau; s)\rangle$ in Eq. (10.6) depends on the longitudinal variable τ; therefore

$$[H_{||}, H_\perp] \neq 0 \ . \tag{10.9}$$

We assume that the perturbation is small and synchro-betatron coupling is avoided. Then

$$[H_{||}, H_\perp] \approx 0 \ . \tag{10.10}$$

This implies that in the transverse phase space, the azimuthal modes $m_\perp = 1,\ 2,\ \cdots$, and the radial modes $k_\perp = 1,\ 2,\ \cdots$ are good eigenmodes. In fact, this is very reasonable because at small perturbation, the transverse azimuthal modes $m_\perp$ correspond to frequencies $m_\perp \omega_\beta$ with separation ω_β. Since

$$\omega_\beta \gg \omega_0 \gg \omega_s \ , \tag{10.11}$$

the possibility for different transverse azimuthals to couple is remote. A direct result of Eq. (10.10) is the factorization of the bunch distribution Ψ in the combined longitudinal-transverse phase space; i.e.,

$$\Psi(r, \phi; r_\beta, \theta) = \psi(r, \phi) f(r_\beta, \theta) \ , \tag{10.12}$$

where $\psi(r,\phi)$ is the distribution in the longitudinal phase space and $f(r_\beta,\theta)$ the distribution in the transverse phase space. Now decompose ψ and f into the unperturbed parts and the perturbed parts:

$$\begin{aligned}\psi(r,\phi) &= \psi_0(r)+\psi_1(r,\phi)\ ,\\ f(r_\beta,\theta) &= f_0(r_\beta)+f_1(r_\beta,\theta)\ .\end{aligned} \tag{10.13}$$

When substituted into Eq. (10.12), there are four terms. The term $\psi_1 f_0$ implies only the longitudinal-mode excitations driven by the longitudinal impedance without any transverse excitations. This is what we have discussed in the previous sections and we do not want to include it again in the present discussion. The term $\psi_0 f_1$ describes the transverse excitations driven by the transverse impedance only. This term will be included in the $\psi_1 f_1$ term if we retain the azimuthal $m=0$ longitudinal mode. For this reason, the bunch distribution Ψ in the combined longitudinal-transverse phase space contains only two terms

$$\Psi(r,\phi;r_\beta,\theta)=\psi_0(r)f_0(r_\beta)+\psi_1(r,\phi)f_1(r_\beta,\theta)e^{-i\Omega s/v}\ , \tag{10.14}$$

where we have separated out the collective angular frequency Ω from $\psi_1 f_1$.

10.3 Sacherer's Integral Equation

The linearized Vlasov equation is studied in the circular coordinates in both the longitudinal phase space and transverse phase space. However, only the transverse wake force will be included in the discussion here. After substituting the distribution in Eq. (10.14), the first order terms of the equation become

$$\left[-i\frac{\Omega}{v}f_1\psi_1+\frac{\omega_s}{v}f_1\frac{\partial\psi_1}{\partial\phi}+\frac{\omega_\beta}{v}\psi_1\frac{\partial f_1}{\partial\theta}\right]e^{-i\Omega s/v}-\psi_0\frac{df_0}{dr_\beta}\sin\theta\frac{c}{E_0\omega_\beta\beta}\langle F_1^\perp(\tau;s)\rangle=0\ . \tag{10.15}$$

It is worth pointing out that since the transverse wake force $\langle F_1^\perp(\tau;s)\rangle$ is a function of the longitudinal coordinate τ, it should also contribute to the second equation of Eq. (9.2) although the longitudinal wake force has been neglected here. It is, however, legitimate to drop this contribution if synchro-betatron resonance is avoided and the transverse beam size has not grown too large (see Exercise 10.4).

The next approximation is to consider only the rigid dipole mode in the transverse phase space; i.e., the bunch is displaced by an infinitesimal amount D from the center

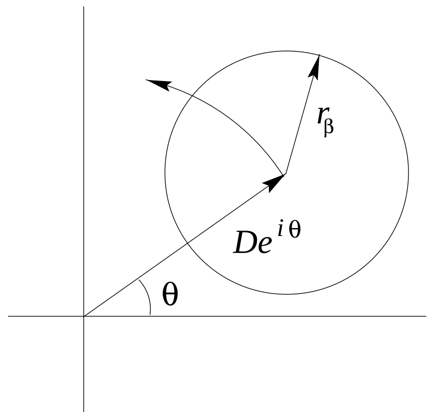

Figure 10.1: A bunch executing betatron motion with an amplitude D in the rigid dipole mode. In the transverse phase space, it is rotating counterclockwise rigidly with the radial offset D.

of the transverse phase space and executes betatron oscillations as a rigid object by revolving at frequency $\omega_\beta/(2\pi)$ counterclockwise. Then according to the convention of Eq. (10.5) and Fig 10.1, we must have,

$$f_0(r_\beta) + f_1(\vec{r}_\beta) = f_0\left(\vec{r} - De^{i\theta}\right) \ , \tag{10.16}$$

where $\vec{r}_\beta$ and $\vec{r}$ are treated as complex number in the transverse phase plane. When $D \to 0$, this becomes

$$f_1(r_\beta, \theta) = -Df_0'(r_\beta)e^{i\theta} \ . \tag{10.17}$$

Since we are retaining only one mode of transverse motion, all the modes that we are going to study are again synchrotron motion on top of this transverse mode. For this reasons, these synchrotron modes are no longer sidebands of the revolution harmonics; they are now sidebands of the betatron sidebands. Some of the transverse modes are shown in Fig. 10.2.

Equation. (10.15) then becomes

$$\left[i(\Omega - \omega_\beta)\psi_1 - \omega_s\frac{\partial\psi_1}{\partial\phi}\right] De^{-i\Omega s/v} + \frac{ic^2}{2E_0\omega_\beta}\psi_0\langle F_1^\perp(\tau; s)\rangle = 0 \ , \tag{10.18}$$

where we have dropped the $e^{-i\theta}$ component of $\sin\theta$ because that corresponds to rotation in the transverse phase space with frequency $-\omega_\beta/(2\pi)$ which is very far from $\omega_\beta/(2\pi)$ provided that the frequency shift due to the wake force is small. Notice that the transverse distribution $f_1(r_\beta, \theta)$ has been removed and the Vlasov equation involves only the

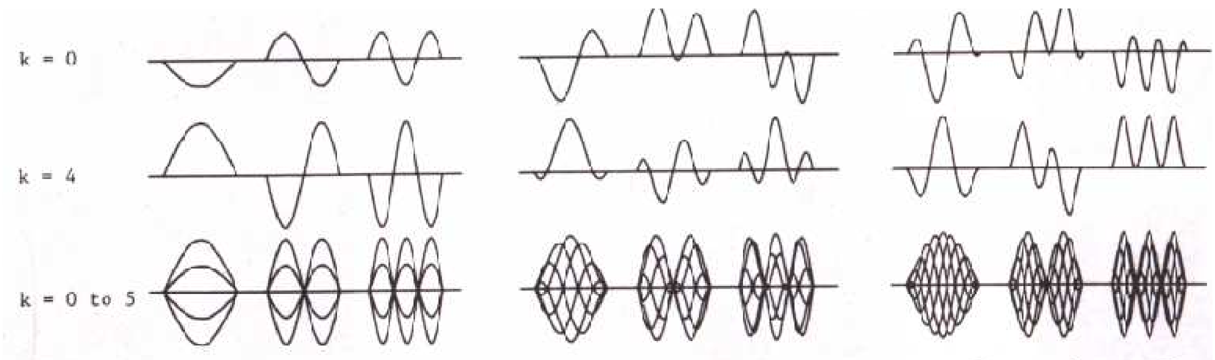

mode $m\!=\!0$ $m\!=\!\pm1$ $m\!=\!\pm2$ $m\!=\!0$ $m\!=\!\pm1$ $m\!=\!\pm2$ $m\!=\!0$ $m\!=\!\pm1$ $m\!=\!\pm2$

(a) $\chi\!=\!0$ rad (b) $\chi\!=\!5$ rad (c) $\chi\!=\!9$ rad

Figure 10.2: Head-tail modes of transverse oscillation. The plots show the contortions of a single bunch on separate revolutions, and with six revolutions superimposed (denoted by k). Vertical axis is difference signal from position monitor, horizontal axis is time, and $\nu_\beta = 4.833$. The chromaticity phases are (a) $\chi = 0$ rad, (b) $\chi = 5$ rad, and (c) $\chi = 9$ rad. Chromaticity will be introduced in Sec. 10.6.

longitudinal perturbed distribution function $\psi_1(r,\phi)$. This ψ_1 is the same perturbed distribution that we studied before with the exception that the azimuthal mode $m=0$ is included.

The transverse wake force on a beam particle in the nth bunch at a time advance τ is, similar to the longitudinal counterpart in Eq. (9.9),

$$\begin{aligned}\langle F_{1n}^{\perp}(\tau;s)\rangle = -\frac{e^2D}{C}\sum_{k=-\infty}^{\infty}\sum_{\ell=0}^{M-1}\int_{-\infty}^{\infty}d\tau'\times \\ \times\,\rho_\ell[\tau';s-kC-(s_\ell-s_n)-v(\tau'-\tau)]W_1[kC+(s_\ell-s_n)+v(\tau'-\tau)]\,. \qquad (10.19)\end{aligned}$$

We assume M identical bunches equally spaced. For the μth coupled mode, we substitute in the above expression the perturbed density of the nth bunch $\rho_{1n}(\tau)e^{-i\Omega s/v}$ including the phase lead as given by Eq. (9.10). Now the derivation follows exactly the longitudinal counterpart in Chapter 9 and we obtain

$$\langle F_{1n\mu}^{\perp}(\tau;s)\rangle = \frac{ie^2MD\omega_0\beta}{C}\,e^{-i\Omega s/v}\sum_{q=-\infty}^{\infty}\tilde\rho_{1n}(\omega_q)Z_1^{\perp}(\omega_q)e^{i\omega_q\tau}\;, \qquad (10.20)$$

where $\omega_q = (qM+\mu)\omega_0+\omega_\beta+\Omega$. We next substitute the result into the linearized Vlasov equation and expand ψ_1 into azimuthals according to $\psi_1(r,\phi)=\sum_m \alpha_m R_m(r)e^{im\phi}$. We finally obtain Sacherer's integral equation for transverse instability

$$(\Omega-\omega_\beta-m\omega_s)\alpha_m R_m(r)= \\ -\frac{i\pi e^2MNc}{E_0\omega_\beta T_0^2}\,g_0\sum_{m'}i^{m-m'}\alpha_{m'}\int r'dr'R_{m'}(r')\sum_q Z_1^\perp(\omega_q)J_{m'}(\omega_q r')J_m(\omega_q r)\,, \quad (10.21)$$

where the unperturbed distribution $g_0(r)$ defined in Eq. (9.30) has been used instead of $\psi_0(r)$. Notice that all transverse distributions are not present in the equation and what we have are longitudinal distributions. This is not unexpected because we have retained only one transverse mode of motion, namely the rigid dipole mode, in the transverse phase space. Therefore, the Sacherer's integral equation for transverse instability is almost the same as the one for longitudinal instability. There are only two differences. First, the unperturbed longitudinal distribution $g_0(r)$ appears in the former but $r^{-1}dg_0(r)/dr$ appears in the latter. Second, although the $m=0$ mode does not occur in the longitudinal equation because of violation of energy conservation, however, it is a valid azimuthal mode in the transverse equation because it describes rigid betatron oscillation.

10.4 Solution of Sacherer's Integral Equations

Consider first the transverse integral equation, where $W(r)=g_0(r)$ is considered to be a weight function. For each azimuthal m, find a complete set of orthonormal functions $g_{mk}(r)$ $(k=1,\ 2,\ \cdots)$ such that

$$\int W(r)g_{mk}(r)g_{mk'}(r)rdr=\delta_{kk'}\ . \quad (10.22)$$

On both sides of the integral equation, perform the expansion

$$\alpha_m R_m(r)e^{im\phi}=\sum_k a_{mk}W(r)g_{mk}(r)e^{im\phi}\ . \quad (10.23)$$

Some comments are necessary. From Eq. (10.22), it appears that the orthonormal functions $g_{mk}(r)$ depend on the weight function $W(r)$ only and are independent of the azimuthal m. As a result, $g_{mk}(r)$ will not be uniquely defined, because the weight function $W(r)=g_0(r)$ is independent of m. In fact, this is not true. If we look into either the Sacherer's longitudinal integral equation (9.31) or the transverse integral equation (10.21) for one single azimuthal, it is easy to see that

$$R_m(r) \propto W(r) J_m(\omega_q r) \ . \tag{10.24}$$

Therefore, for small r, we must have the behavior

$$R_m(r) \sim r^m \lim_{r\to 0} W(r) \ . \tag{10.25}$$

Taking the parabolic distribution in the longitudinal case as an example, $\lim_{r\to 0} W(r)$ is a constant implying that $R_m(r) \sim r^m$. From Eq. (10.23), since $g_{mk}(r)$ is the expansion of $R_m(r)$, the small-r behavior of $g_{mk}(r)$ will be constrained. This makes the set of orthonormal functions $g_{mk}(r)$ dependent on the azimuthal m and become, in fact, unique.

After substituting the expansion of $\alpha_m R_m$ into both sides of Eq. (10.21), multiply on both sides by $g_{mk}(r)$ and integrate over rdr. Sacherer's integral equation becomes

$$(\Omega - \omega_\beta - m\omega_s) a_{mk} = -\frac{i\pi e^2 MNc}{E_0 \omega_\beta T_0^2} \sum_{m'k'} a_{m'k'} \sum_q Z_1^\perp(\omega_q) \tilde{\lambda}^*_{mk}(\omega_q) \tilde{\lambda}_{m'k'}(\omega_q) \ , \tag{10.26}$$

where we have defined

$$\tilde{\lambda}_{mk}(\omega) = \int i^{-m} W(r) J_m(\omega r) g_{mk}(r) r dr \ . \tag{10.27}$$

The $\tilde{\lambda}_{mk}(\omega)$ is the Fourier transform of the eigenmode $\lambda_{mk}(\tau)$, which can be shown to be in fact the (mk) component of the perturbed linear density $\rho_1(\tau)$. Let us start from the Fourier transform of the linear density of the (mk)th mode

$$\tilde{\rho}_1^{(mk)}(\omega) = \frac{1}{2\pi} \int d\tau \rho_1^{(mk)}(\tau) e^{-i\omega\tau} = \frac{1}{2\pi} \int d\tau d\Delta E \, \psi_1^{(mk)}(\tau, \Delta E) e^{-i\omega\tau} \ . \tag{10.28}$$

Now substitute the (mk)th mode of Eq. (10.23) for $\psi_1^{(mk)}$ to obtain

$$\tilde{\rho}_1^{(mk)}(\omega) = \frac{\omega_s \beta^2 E_0}{2\pi\eta} \int r dr d\phi \, W(r) g_{mk}(r) e^{im\phi - i\omega\tau} \ . \tag{10.29}$$

The integration over ϕ can be performed to yield a Bessel function. Finally using the definition of $\tilde{\lambda}_{mk}(\omega)$ given in Eq. (10.27), we arrive at

$$\tilde{\rho}_1^{(mk)}(\omega) = \frac{\omega_s \beta^2 E_0}{\eta} \int r dr \, W(r) g_{mk}(r) i^{-m} J_m(\omega r) = \frac{\omega_s \beta^2 E_0}{\eta} \tilde{\lambda}_{mk}(\omega) \ . \tag{10.30}$$

Taking the Fourier transform, we therefore obtain

$$\rho_1^{(mk)}(\tau) = \frac{\omega_s \beta^2 E_0}{\eta} \lambda_{mk}(\tau) \ . \tag{10.31}$$

Notice that $\tilde{\lambda}_{mk}(\omega)$ is dimensionless; therefore it must be a function of $\omega\tau_L$ where τ_L is the total bunch length. The sum over the power spectrum should give us

$$\sum_q |\tilde{\lambda}_{mk}(\omega_q)|^2 \approx \int \frac{d\omega}{M\omega_0} |\tilde{\lambda}_{mk}(\omega)|^2 \sim \frac{1}{M\omega_0 \tau_L} \ , \tag{10.32}$$

where $\omega_q = (qM + \mu)\omega_0 + \omega_\beta + m\omega_s$. For this reason, Eq. (10.26) can roughly be transformed into

$$(\Omega - \omega_\beta - m\omega_s) a_{mk} = -\frac{i}{1+m} \frac{e\beta c^2}{2\omega_\beta E_0} \frac{I_b}{L} \sum_{m'k'} a_{m'k'} \frac{\sum_q Z_1^\perp(\omega_q) \tilde{\lambda}_{mk}^*(\omega_q) \lambda_{m'k'}(\omega_q)}{\sum_q \tilde{\lambda}_{mk}^*(\omega_q) \lambda_{mk}(\omega_q)} \ , \tag{10.33}$$

where I_b is the current of one bunch and $L = \beta c \tau_L$ is the total bunch length. Equation (10.33) is especially useful if we include only one mode of excitation. For example, the lowest radial mode $k = 1$ is usually the most prominent one to be excited and the different azimuthal modes do not mix when the perturbation is small.

This expression is very similar to the coasting-beam formula of Eq. (10.4). Besides the averaging over the power spectra, the coasting beam current per unit length I_0/C is replaced by the average single bunch current I_b divided by the total bunch length L in meters. The factor $(1+m)^{-1}$ in front says that higher-order modes are harder to excite, and is introduced under some assumption of the unperturbed distribution in phase space [2]. It is easy to understand why the power spectrum $h_{mk}(\omega) = |\tilde{\lambda}_{mk}(\omega)|^2$ enters because $Z_1^\perp(\omega)\tilde{\lambda}_{mk}(\omega)$ gives the deflecting field, which must be integrated over the bunch spectrum to get the total force. Written in the form of Eq. (10.33), there is no need for $\tilde{\lambda}_{mk}(\omega)$ or $\lambda_{mk}(\tau)$ to have any special normalization.

The Sacherer's longitudinal integral equation (9.29) can be solved in exactly the same way by identifying the weight function as

$$W(r) = -\frac{1}{r} \frac{dg_0(r)}{dr} \ , \tag{10.34}$$

where the negative sign is included because $dg_0(r)/dr < 0$. The result is

$$(\Omega - m\omega_s) a_{mk} = \frac{i2\pi e^2 MNm\eta}{\beta^2 E_0 T_0^2 \omega_s} \sum_{m'k'} a_{m'k'} \sum_q \frac{Z_0^\parallel(\omega_q)}{\omega_q} \tilde{\lambda}_{mk}^*(\omega_q) \tilde{\lambda}_{m'k'}(\omega_q) \ , \tag{10.35}$$

where $\tilde{\lambda}_{mk}(\omega_q)$ is again given by Eq. (10.27), but with the weight function replaced by Eq. (10.34). However, $\tilde{\lambda}_{mk}(\omega_q)$ now has the dimension of of $(\text{time})^{-1}$ because the weight function is different. Dimensional analysis gives

$$\sum_q |\tilde{\lambda}_{mk}(\omega_q)|^2 \approx \int \frac{d\omega}{M\omega_0} |\tilde{\lambda}_{mk}(\omega)|^2 \sim \frac{1}{M\omega_0 \tau_L^3} \ . \tag{10.36}$$

Equation (10.35) becomes approximately

$$(\Omega - m\omega_s) a_{mk} = \frac{im}{1+m} \frac{4\pi^2 e I_b \eta}{3\beta^2 E_0 \omega_s \tau_L^3} \sum_{m'k'} a_{m'k'} \frac{\sum_q \dfrac{Z_0^{\|}(\omega_q)}{\omega_q} \tilde{\lambda}_{m'k'}(\omega_q) \tilde{\lambda}^*_{mk}(\omega_q)}{\sum_q \tilde{\lambda}^*_{mk}(\omega_q) \tilde{\lambda}_{mk}(\omega_q)} \ , \tag{10.37}$$

where the extra factor in front is a result of the assumption of some particular unperturbed phase-space distribution. A more detailed derivation of Eq. (10.37) can be found in Ref. [2].

10.5 Sacherer's Sinusoidal Modes

Assuming the perturbation is small so that only a single azimuthal mode will contribute, we learn from the Sacherer's integral equation (10.21) that the perturbed excitation is

$$R_m(r) e^{im\phi} \propto W(r) J_m(\omega_q r) e^{im\phi} \ . \tag{10.38}$$

For a bunch of half length $\hat{\tau} = \frac{1}{2}\tau_L$, $R_m(\hat{\tau}) = 0$. So it is reasonable to write the kth radial mode corresponding to azimuthal m as

$$R_{mk}(r) e^{im\phi} \propto W(r) J_m\left(x_{mk} \frac{r}{\hat{\tau}}\right) e^{im\phi} \ , \tag{10.39}$$

where x_{mk} is the kth zero of the Bessel function J_m. Sacherer [3] discovered that, assuming a uniform or water-bag unperturbed distribution; i.e., $W(r)$ is constant for $r < \hat{\tau}$, the projection of $R_{mk}(r)e^{im\phi}$ onto the τ axis

$$\rho_{(mk)}(\tau) \propto \int W(r) J_m\left(x_{mk} \frac{r}{\hat{\tau}}\right) e^{im\phi} d\Delta E \tag{10.40}$$

is approximately sinusoidal. In fact, head-tail excitations that are sinusoidal-like had been observed in the CERN Proton Synchrotron (PS) booster. For this reason, instead of solving the integral equation, Sacherer approximated $\rho_{(mk)}(\tau)$ by a linear combination of sinusoidal functions, and these modes are called sinusoidal modes. He introduced a set of orthonormal functions

$$\lambda_m(\tau) \propto \begin{cases} \cos(m+1)\pi\dfrac{\tau}{\tau_L} & m = 0, 2, \cdots, \\ \sin(m+1)\pi\dfrac{\tau}{\tau_L} & m = 1, 3, \cdots. \end{cases} \tag{10.41}$$

Note that $\lambda_m(\tau)$ has exactly m nodes along the bunch not including the two ends. If we restrict ourselves to the most prominent lowest radial mode ($k = 1$), these $\lambda_m(\tau)$'s are just the approximates to $\rho_{(m1)}(\tau)$. From now on, the radial mode index k will be dropped.

The power spectrum of the modes in Eq. (10.41) is proportional to

$$h_m(\omega) = \frac{4(m+1)^2}{\pi^2}\frac{1+(-1)^m\cos\pi y}{[y^2-(m+1)^2]^2} \tag{10.42}$$

where $y = \omega\tau_L/\pi$ and $\tau_L = L/v$ is the total length of the bunch in time. They are plotted in Fig. 7.5. The normalization of $h_m(\omega)$ in Eq. (10.42) has been chosen in such a way that, when the smooth approximation is applied to the summation over k, we have

$$B\sum_{q=-\infty}^{+\infty} h_m(\omega_q) \approx \frac{B}{M\omega_0}\int_{-\infty}^{+\infty} h_m(\omega)d\omega = 1\ . \tag{10.43}$$

Here $B = M\omega_0\tau_L/(2\pi)$ is the bunching factor in the presence of M identical equally-spaced bunches, or the ratio of full bunch length to bunch separation.

For the elliptical distribution in the longitudinal phase space, $g_0(r) \propto (\hat{\tau}^2 - r^2)^{-1/2}$, so that the linear density becomes constant, the spectral excitations of the lowest radial mode $\lambda_m(\tau)$ are the Legendre polynomials, the Fourier transform $\tilde{\lambda}_m(\omega)$ are the spherical Bessel functions j_m, and the power spectra $h_m \propto |j_m|^2$. We called these the Legendre modes. For the bi-Gaussian distribution in the longitudinal phase space, $\lambda_m(\tau)$ are the Hermite polynomials and $\tilde{\lambda}_m(\omega)$ are ω^m multiplied by a Gaussian. We call these the Hermite modes.

For the longitudinal integral equation, we have the same modes if we have the same weight function. For the longitudinal case, the weight function is $W(r) = g_0'(r)/r$ instead. Therefore the sinusoidal modes correspond to $g_0(r) \propto (\hat{\tau}^2 - r^2)$ or linear density

$\rho(\tau) \propto (\hat{\tau}^2 - \tau^2)^{3/2}$. The Legendre modes correspond to $g_0(r) \propto (\hat{\tau}^2 - r^2)^{1/2}$ or parabolic linear density $\rho(\tau) \propto (\hat{\tau}^2 - \tau^2)$. The Hermite modes correspond to the same bi-Gaussian distribution as in the transverse situation. These solutions are summarized in Table 10.1.

Sometimes the growth rates computed are rather sensitive to the longitudinal bunch distribution assumed. Therefore, results using the sinusoidal modes are estimates only.

After so much mathematics, it is possible to present some simple expressions for the growth rates. From Eq. (10.37) for the longitudinal and Eq. (10.33) for the transverse, let us assume that there is no mixing between azimuthal modes as well as radial modes. Then the longitudinal growth rate simplifies to

$$\frac{1}{\tau_{mk\mu}} = \mathcal{I}m\,\Omega \approx \frac{m}{1+m}\,\frac{4\pi^2 eI_b\eta}{3\beta^2E_0\omega_s\tau_L^3}\sum_q \frac{\mathcal{R}e\,Z_0^{\|}(\omega_q)}{\omega_q}h_{mk}(\omega_q)\ , \tag{10.44}$$

where $\omega_q = (qM+\mu)\omega_0 + m\omega_s$ and the power spectrum has been normalized to unity according to Eq. (10.43). The transverse growth rate simplifies to

$$\frac{1}{\tau_{mk\mu}} = \mathcal{I}m\,\Omega \approx -\frac{1}{1+m}\,\frac{eI_bc}{4\pi\nu_\beta E_0}\sum_q \mathcal{R}e\,Z_1^{\perp}(\omega_q)h_{mk}(\omega_q)\ , \tag{10.45}$$

where $\omega_q = (qM+\mu)\omega_0 + \omega_\beta + m\omega_s$.

10.6 Chromaticity Frequency Shift

The betatron tune ν_β of a beam particle depends on its momentum offset δ. The chromatic betatron tune shift is defined as

$$\Delta\nu_\beta = \xi\delta\ , \tag{10.46}$$

where ξ is called the *chromaticity**. Because the beam particle makes synchrotron oscillations, its betatron tune will be changing from turn to turn depending on its momentum offset. There will be a betatron phase offset which will accumulate. Consider a beam particle which is currently at the head of the bunch. It will be executing betatron oscillations with the same betatron tune as the synchronous particle, because it is at the synchronous momentum. Below transition, the synchrotron oscillation is clockwise in

*Sometimes, especially in Europe, the chromaticity ξ is also defined by $\Delta\nu_\beta = \xi\nu_\beta\delta$.

Table 10.1: Some solutions of the Sacherer's integral equations for longitudinal and transverse excitations with only one radial mode included in each case.

Longitudinal Integral Equation		Transverse Integral Equation		Weight Function	Azimuthal Excitation Modes	
Phase-space Distribution	Linear Distribution	Phase-space Distribution	Linear Distribution	$W(r)$	Linear Distribution	Spectral Distribution
$f_0(r)$	$\lambda(\tau)$	$g_0(r)$	$\lambda(\tau)$	$\sim g_0(r) \sim \dfrac{f_0'(r)}{r}$	$\lambda_{m1}(\tau)$	$\tilde{\lambda}_{m1}(\omega)$
Water-bag $H(\hat{\tau}-r)$	$\sqrt{\hat{\tau}^2-\tau^2}$	Air-bag $\delta(\hat{\tau}-r)$	$\dfrac{1}{\sqrt{\hat{\tau}^2-\tau^2}}$	$\delta(\hat{\tau}-r)$	$\dfrac{T_m(\tau/\hat{\tau})}{\sqrt{1-(\tau/\hat{\tau})^2}}$	$J_m(\omega\hat{\tau})$
$\hat{\tau}^2-r^2$	$(\hat{\tau}^2-\tau^2)^{\frac{3}{2}}$	constant	$\sqrt{\hat{\tau}^2-\tau^2}$	constant	sinusoidal	$\sqrt{h_m(\omega)}$ of Eq. (10.42)
$\sqrt{\hat{\tau}^2-r^2}$	$\hat{\tau}^2-\tau^2$	$\dfrac{1}{\sqrt{\hat{\tau}^2-r^2}}$	constant	$\dfrac{1}{\sqrt{\hat{\tau}^2-r^2}}$	$P_m(\tau/\hat{\tau})$	$j_m(\omega\hat{\tau})$
$e^{-\frac{r^2}{2\sigma^2}}$	$e^{-\frac{\tau^2}{2\sigma^2}}$	$e^{-\frac{r^2}{2\sigma^2}}$	$e^{-\frac{\tau^2}{2\sigma^2}}$	$e^{-\frac{r^2}{2\sigma^2}}$	$H_m\left(\frac{\tau}{\sqrt{2}\sigma}\right)$	$(\omega\sigma)^m e^{-\frac{\omega^2}{2\sigma^2}}$

the longitudinal phase space as indicated in Fig. 10.3, because, for example, at a positive momentum offset, the particle comes back earlier or its arrival time advance increases. Thus leaving the head of the bunch, the particle loses energy and starts to oscillate

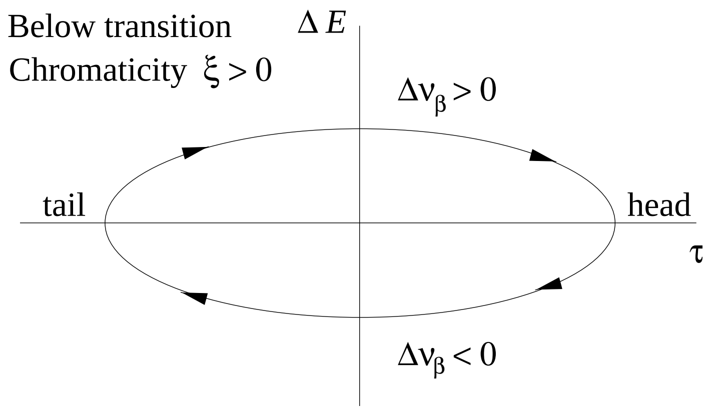

Figure 10.3: Synchrotron motion in the longitudinal phase space below transition. If chromaticity ξ is positive, the betatron tune will be larger/smaller than that of the synchrotron particle, when the particle energy offset is positive/negative.

with smaller betatron tune if the chromaticity ξ is positive. Turn by turn, the slip in betatron phase accumulates and reaches a maximum when the particle arrives at the tail of the bunch. After that the momentum offset of the second half of the synchrotron oscillation becomes positive. The betatron tune is larger than the nominal value and the accumulated betatron phase slip gradually reduces. When the particle arrives at the head all the betatron phase slip vanishes. This phase slip is illustrated schematically in Fig. 10.4.

We would like to compute the phase slip for a particle that has a time advance τ relative to the synchronous particle. The momentum offset in Eq. (10.46) can be eliminated using the equation of motion of the phase

$$\Delta\tau = -\eta T_0 \delta \ , \tag{10.47}$$

where η is the slip factor and $\Delta\tau$ is the change in time advance of the particle in a turn. The phase lag in a turn is then

$$\int 2\pi\Delta\nu_\beta = -2\pi\frac{\xi}{\eta}\int\frac{\Delta\tau}{T_0} = -\frac{\xi\omega_0}{\eta}\tau \ . \tag{10.48}$$

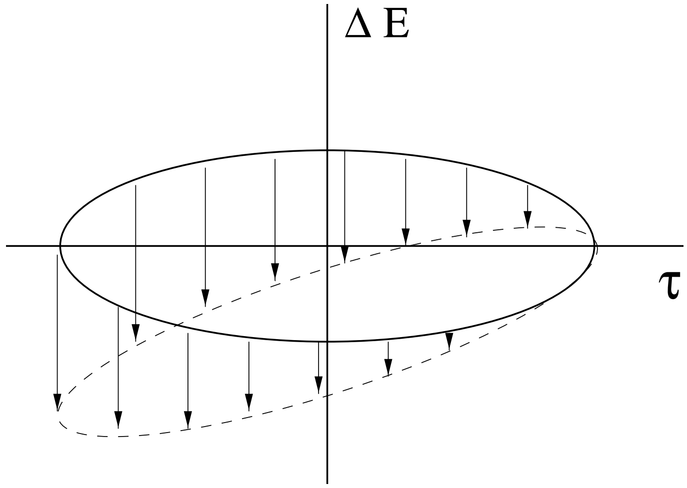

Figure 10.4: Schematic drawing showing the lagging of the betatron phase, depicted by the arrows, from the head (right) to the tail (left) of the bunch when the chromaticity ξ and slip factor η have the same signs.

Thus, below transition ($\eta < 0$), a particle at the bunch head ($\tau = \hat{\tau}$) has an accumulated betatron phase advance of $-\xi\omega_0\hat{\tau}/\eta$ relative to the synchronous particle, while a particle at the tail ($\tau = -\hat{\tau}$) has an accumulated betatron phase slip of $-\xi\omega_0\hat{\tau}/\eta$. Equation (10.48) indicates that the phase lag increases linearly along the bunch and is independent of the momentum offset. Relative to the synchronous particle, we write this accumulated betatron phase for a particle at arrival time advance τ as

$$-\frac{\xi\omega_0}{\eta}\tau = -\omega_\xi\tau \ , \tag{10.49}$$

where

$$\omega_\xi = \frac{\xi\omega_0}{\eta} \tag{10.50}$$

is called the *betatron angular frequency shift due to chromaticity.* Below transition and for positive chromaticity, ω_ξ is negative, but the accumulated betatron phase at the bunch head is positive. Thus, in previous derivation we should make the substitution

$$e^{i\omega_q\tau} \to e^{i(\omega_q-\omega_\xi)\tau} \ . \tag{10.51}$$

where $\omega_q = (qM+\mu)\omega_0 + m\omega_s$. For this reason, ω_ξ should be subtracted from ω_q in the argument of the power spectrum h_m but not in the argument of $\mathcal{R}e\, Z_1^\perp$ of the growth rate formula like Eq. (10.45) and also not in the argument of $\mathcal{I}m\, Z_1^\perp$ of the tune shift formula. The total betatron phase shift from head to tail is represented by $\chi = \omega_\xi\tau_L$,

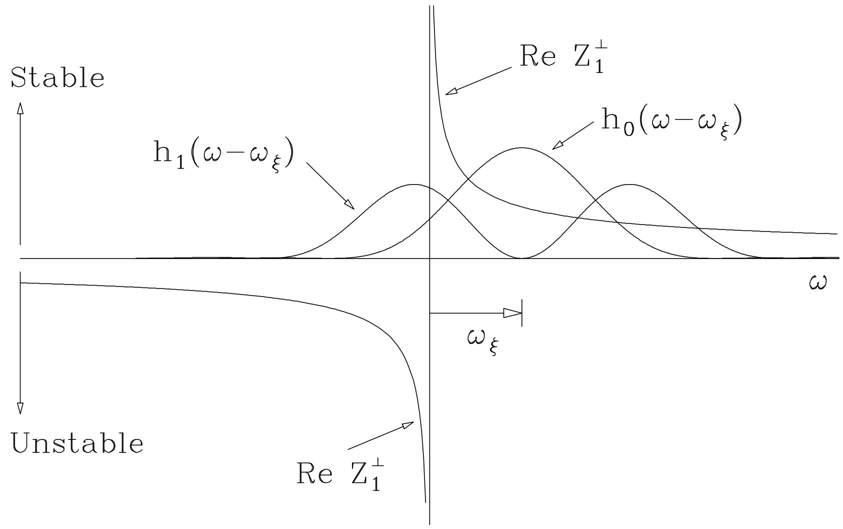

Figure 10.5: Positive chromaticity above transition shifts the all modes of excitation towards the positive frequency side by ω_ξ. Mode $m = 0$ becomes stable, but mode $m = 1$ may be unstable because it samples more negative $\mathcal{R}e\, Z_1^\perp$ than positive $\mathcal{R}e\, Z_1^\perp$.

where τ_L is the total length of the bunch from head to tail. The head-tail modes for various values of χ are shown in Fig. 10.2.

For positive chromaticity above transition, $\omega_\xi > 0$, the modes of excitation in Fig. 7.5 are therefore shifted to the right by the angular frequency ω_ξ. As shown in Fig. 10.5, mode $m = 0$ sees more impedance in positive frequency than negative frequency and is therefore stable. However, it is possible that mode $m = 1$, as in the illustration of Fig. 10.5, samples more the highly negative $\mathcal{R}e\, Z_1^\perp$ at negative frequencies than positive $\mathcal{R}e\, Z_1^\perp$ at positive frequencies and becomes unstable.

If the transverse impedance is sufficiently smooth, it can be removed from the summation in Eq. (10.45). The growth rate for the $m = 0$ mode becomes

$$\frac{1}{\tau_0} = -\frac{eI_bc}{2\omega_\beta E_0 \tau_L}\, \mathcal{R}e\, Z_1^\perp(\omega_\xi) \ . \tag{10.52}$$

The transverse impedance of the CERN Proton Synchrotron (PS) had been measured in this way by recording the growth rates of a bunch at different chromaticities.

10.7 Exercises

10.1. Fill in all the steps in the derivation of Sacherer's integral equation for transverse instabilities.

10.2. Derive the power spectra of the sinusoidal modes of excitation in Eq. (10.41), and show that they are given by Eq. (10.42) when properly normalized according to Eq. (10.43).

10.3. If the transverse impedance is sufficiently smooth, it can be removed from the summation in Eq. (10.33). Show that the growth rate for the $m = 0$ mode becomes

$$\frac{1}{\tau_0} = -\frac{eI_b c}{2\omega_\beta E_0 \tau_L} \mathcal{R}e\, Z_1^\perp(\omega_\xi) \ . \tag{10.53}$$

The transverse impedance of the CERN PS has been measured in this way by recording the growth rates of a bunch at different chromaticities. The CERN PS has a mean radius of 100 m and it can store proton bunches from 1 to 26 GeV with a transition gamma of $\gamma_t = 6$. The bunch has a spectral spread of $\sim \pm 100$ MHz, implying that each measurement of the impedance is averaged over an interval of $\sim$ 200 MHz. If the impedance has to be measured up to $\sim$ 2 GHz and the sextupoles in the PS can attain chromaticities in the range of ± 10, at what proton energy should this experiment be carried out?

10.4. Redefine the longitudinal coordinates in Eq. (9.1) by $X = xv$ and $P_X = p_x v$, where v is the particle velocity, so that X carries the dimension of length.

(a) Show that, for the equations of motion (9.2) in the longitudinal phase space and (10.6) in the transverse phase space, the Hamiltonian is

$$\begin{aligned} H = &-\frac{\omega_s}{2v}(X^2 + P_X^2) - \frac{\omega_\beta}{2v}(y^2 + p_y^2) \\ &- \frac{v\eta}{E_0 \omega_s \beta^2} \int_0^X dX' \langle F_0^{\parallel}(X'/v; s)\rangle + \frac{cy}{E_0 \omega_\beta \beta^2} \langle F_1^\perp (X/v; s)\rangle \ . \end{aligned} \tag{10.54}$$

(b) Show that the second equation of motion in Eq. (9.2) needs to be modified to

$$\frac{dp_x}{ds} = \frac{\omega_s}{v} x + \frac{\eta}{E_0 \omega_s \beta^2} \langle F_0^{\parallel}(x; s)\rangle - \frac{y}{E_0 \omega_\beta \beta^3 v} \frac{\partial}{\partial x} \langle F_1^\perp (x; s)\rangle \ , \tag{10.55}$$

where the last term is the synchro-betatron coupling term which we dropped in our discussion.

Bibliography

[1] E.D. Courant and H.S. Synder, *Theory of the Alternating-Gradient Synchrotron*, Annals of Physics **3**, 1 (1958).

[2] See for example, J.L. Laclare, *Bunch-Beam Instabilities, —Memorial Talk for F.J. Sacherer*, Proc. 11th Int. Conf. High-Energy Accelerators, Geneva, July 7-11, 1980, p. 526.

[3] F.J. Sacherer, *Methods for Computing Bunched-Beam Instabilities*, CERN Report CERN/SI-BR/72-5, 1972.